MedChemComm

Accepted Manuscript

ROYAL SOCIETY OF CHEMISTRY

www.rsc.org/medchemcomm

Navigating into chemical space between MGCD0103 and SAHA: Novel Histone Deacetylase Inhibitor as a Promising Lead

Xin Zhang†[ab], Peng-Cheng Lv†[ab], Dong-Dong Li [ab], Wei-Ming Zhang*[ab], and Hai-Liang Zhu*[ab]

[a]Nanjing Institute for the Comprehensive Utilization of Wild Plant, Nanjing 210042, People's Republic of China.

[b]State Key Laboratory of Pharmaceutical Biotechnology, Nanjing University, Nanjing 210093, People's Republic of China.

E-mail: zhuhl@nju.edu.cn; Fax: +86-25-8359 2672; Tel: +86-25-8359 2572

† These two authors equally contributed to this paper.

Abstract: Histone deacetylase inhibitors (HDIs) are an increasingly important class of cancer targeted agents. Two kinds of small molecule histone deacetylase inhibitors, mainly employing the motifs of the two known HDAC inhibitors MGCD0103 and SAHA as the basic scaffold, were designed, synthesized and evaluated for the preliminary biological activity. Strikingly, these two compounds regained longer half-life potency as MGCD0103 and retained the non-selectivity for HDAC1 versus HDAC6 derived from SAHA. Together, these two compounds combining both advantage of MGCD0103 and SAHA could be considered as novel histone deacetylase inhibitors in targeted drug development, and possibly anticipated to be more effective under the clinical trials.

Introduction

Histone deacetylases (HDACs) have been proved to be one of the most promising targets in cancer drug development over the past few years[1]. It accurately controls the process of lysine acetylation and deacetylation in the epigenetic field, together with histone acetyl transferases (HATs), finally leading to gene transcription or silencing[2]. In addition, there are 18 members separated into four classes in humans HDAC family, and about 50 nonhistone proteins have been discovered as HDAC substrates[2]. Therefore, the biological interaction map in the centre of HDAC seems to be complicated. While HDAC proteins, particularly class I and II members are more linked to carcinogenesis, the detailed molecular mechanism connecting HDAC activity to cancer has not been yet defined, and the precise function of each isoform in cancer cell remains unclear[3]. However, the recent development of HDAC inhibitors (HDIs) can contribute to the success of cancer therapy, particularly adopting the strategy in combination with other antitumor agents in the clinical trial[4].

So far, at least 16 kinds of HDAC inhibitors are being evaluated under the clinical stage (Figure 5). Among them, the two drugs vorinostat (SAHA, unselective HDAC inhibitors) and romidepsin (FK-228) have been approved by the US Food and Drug Administration for cutaneous T-cell lymphoma in 2006 and 2009, respectively[5, 6]. Although it remains unclear whether selective HDAC inhibitors would provide advantages at the utility and potential therapeutic level when compared to the pan-inhibitor SAHA widely used in clinical trial, selective inhibitors can clearly aid in exploring the molecular mechanism connecting HDAC activity to cancer formation, which might provide a more effective chemotherapy[3]. As expected, the emerging trends at the development of HDAC inhibitors have focused on class-selective or isoform-selective aspect (Figure 1), based on the analysis of recently published HDAC inhibitors paper primarily abstracted from *Journal of Medicinal Chemistry*.

One of highlights in this paper is using fragment-based drug design (FBDD), which has emerged as a powerful strategy in lead discovery[7, 8]. The basis of this approach generally involves screening of a relatively small library of fragments. All fragments used in this paper are cut from clinical drugs and have been proved to be the most optimal. Therefore, the currently process of screening has included lots of SAR

discussions before and our design leads to further optimization of activity and selectivity. According to the canonical framework, most of HDIs could be decomposed into one capping group that interacts with the residues at the entrance of the active site, one linker that lie into the hydrophobic space of the binding site tunnel, and one Zn-binding group (ZBG) able to chelate with the Zn^{2+} at the bottom of the cavity (Figure 1). Almost all the clinical HDAC candidates can contain these above three basic moieties, and each part of the molecules seems to the most optimal fragment as to itself.

Currently, a lot of para-substituted benzohydroxamic acids[9-12] and para-substituted cinnamic hydroxamic acids[13-17] are reported as multipotent HDACs inhibitors and certain of them are being evaluated in clinical trials as anticancer preparations. Based on the information above, it has been hypothesized to develop novel HDIs through modifying the ZBG region among these important clinical HDAC inhibitors. We also observed the differences between MGCD0103 and SAHA in terms of their properties of pharmacology and selectivity for isoform of HDAC proteins. For example, SAHA has a relatively less short half-life in plasma ($t_{1/2}$ = 2 h[18]) than MGCD0103 ($t_{1/2}$ = 9 h[19]). SAHA can inhibit the activity of all 11 known human class I and class II HDACs[20], while MGCD0103 has strong isotype selectivity to HDAC1 and some weak inhibition against HDAC2, -3, and -11[21]. In addition, MGCD0103 could produce multiple responses in both lymphoma and AML clinical trials compared to SAHA[22]. Therefore, as shown in the Figure 1, we have designed and synthesized two new HDAC inhibitors compound **1** and **2** (Scheme 1), by recombining the selective HDAC inhibitor MGCD0103 and pan-HDAC inhibitor SAHA (The detailed procedure is available in design section later, and chemistry section details in Supplementary Information), which were expected to combine the longer half-life potency of MGCD0103 and extensive inhibition against HDACs of SAHA. Their exclusive biological activities were preliminarily illustrated in vitro antiproliferative assay, apoptosis and cell cycle assay, in vitro HDACs inhibition fluorescence assay, in vitro stability assay and immunofluorescence microscopy detection.

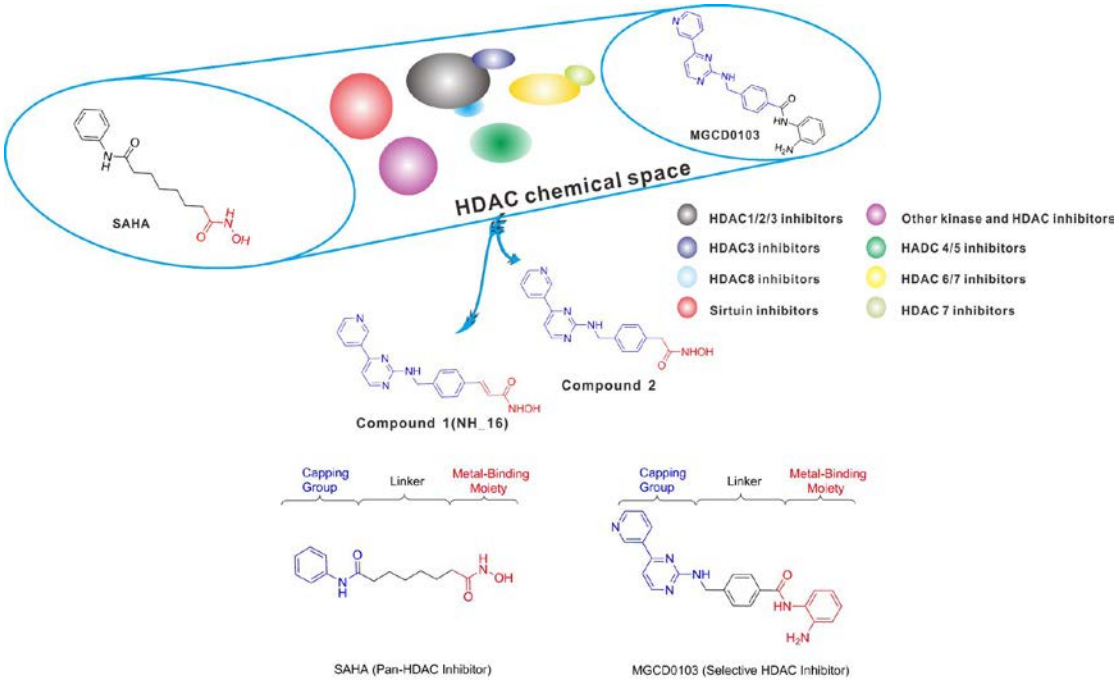

Figure 1

Result and Discussion

In Vitro Antiproliferative Assay

We used 5 common tumor cell lines to investigate the anti-proliferative effect of the two compounds (compound **1** and compound **2**) compared with their templates (MGCD0103 and SAHA) using MTT method. The results revealed that compound **1** and **2** displayed an anti-proliferative effect in time-dependent and dose-dependent manner (Table 1 & Figure s5 in Supplementary Information). The two compounds exhibited better effects than SAHA in A549, Hela, HepG2 and MCF7 cell lines, suggesting they regenerate longer half-life potency by combining the MGCD0103 Capping Group and SAHA Metal-Binding Moiety. Further research will be focused on the stability and comparison of the two compounds and their templates (MGCD0103 and SAHA) in vitro and vivo. Apoptosis and cell cycle arrest could be both contributed to the anti-proliferative effect. Thus it's necessary to investigate the effect of the two compounds on the apoptosis and cell cycle in the following part.

Table 1 Antiproliferative activities of the designed compounds against five common cancer cells

Cancer cells	Compounds	Inhibition IC_{50} (μM)		
		24[a]	48[a]	72[a]
A549	MGCD0103	59.90	14.57	11.87
	SAHA	78.76	5.37	12.46
	1	97.96	8.32	7.99
	2	ND[b]	11.90	4.64
Hela	MGCD0103	43.80	3.32	3.42
	SAHA	7.13	9.19	8.96
	1	53.44	3.79	3.24
	2	30.67	7.23	3.17
HepG2	MGCD0103	5.79	4.05	4.25
	SAHA	10.77	10.52	8.78
	1	20.46	5.95	6.52
	2	22.92	4.03	2.96
HCT116	MGCD0103	29.69	1.24	3.51
	SAHA	32.46	5.06	< 1.18
	1	8.28	< 0.81	1.05
	2	13.70	< 0.88	1.66
MCF-7	MGCD0103	84.17	56.81	2.49
	SAHA	54.55	28.66	9.59
	1	46.03	23.04	2.66
	2	45.98	16.03	2.41

[a]Time incubated with drugs. [b]ND = not determined.

Apoptosis and Cell cycle Assay

HDIs could elicit a number of biological effects on cancer cells, such as apoptosis and cell-cycle arrest. Interestingly, compounds **1** and **2** induced apoptosis in Hela cells in a dose-dependent manner as well as MGCD0103 and SAHA. At higher concentration of 5 μM, these two compounds exhibited a better pro-apoptotic effect than SAHA, although there was a little difference between MGCD0103 and the two compounds (Figure 2). Cell cycle profiles of Hela treated with compounds **1** and **2** by

flow cytometry demonstrated that both of them can induce the G1 phase arrest in which there is a significant G1-phase increase and S-phase decrease with the increase of drug concentration. In addition, it was notable that both compounds could also give rise to an obvious G2-phase decrease at a high concentration (2 μM, Figure 3).

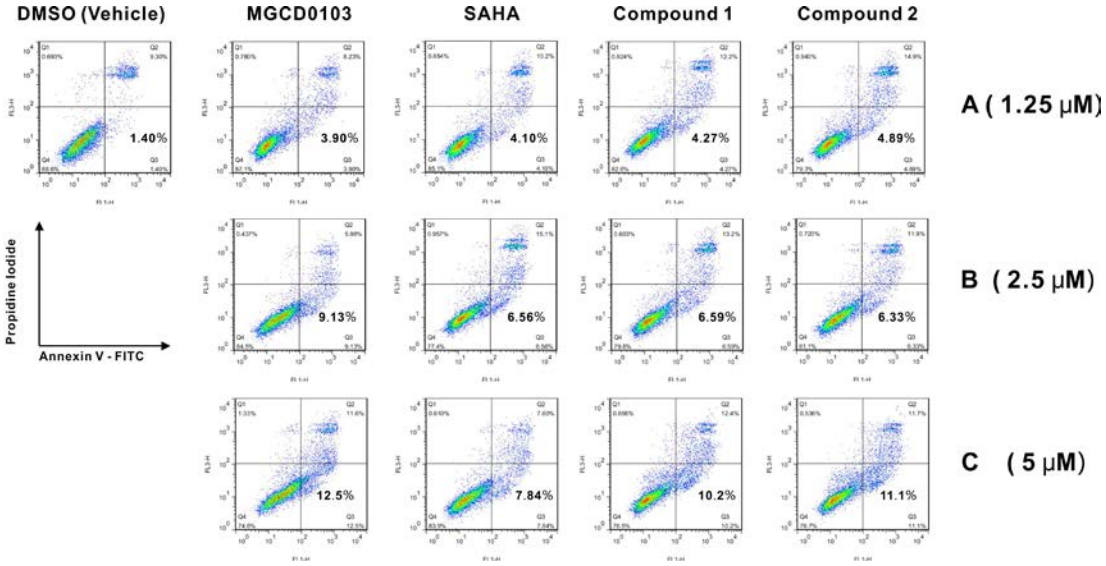

Figure 2

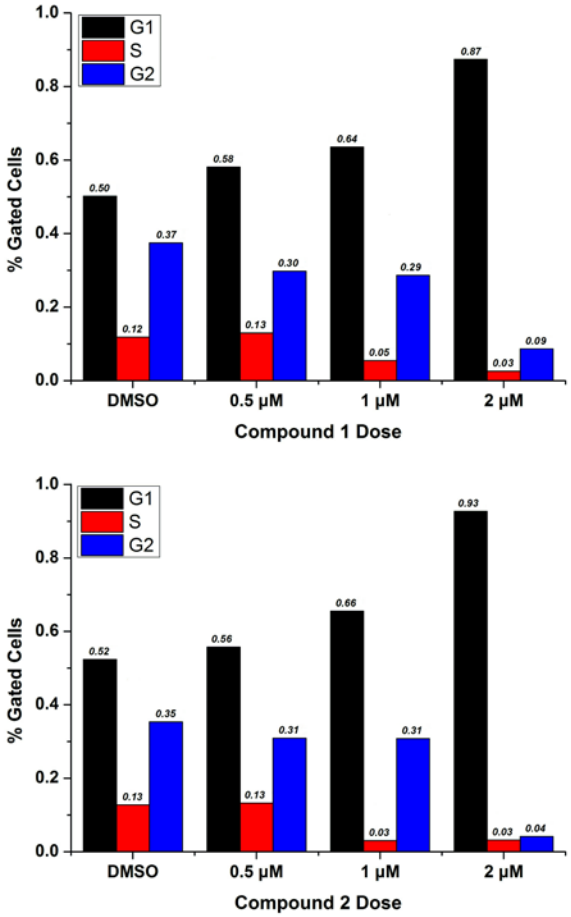

Figure 3

Vitro HDACs Inhibition Fluorescence Assay

The selectivity issue between MGCD0103 and SAHA commonly lay at the inhibition of HDAC6 protein, and *Stuart L. Schreiber* identified that the o-aminoanilide element within HDIs could render such inhibitors inactive toward HDAC6 in cells[23]. Nevertheless, the individual modification of the capping group and linker could also disturb the selectivity of HDIs, and more importantly, we cannot ignore the combination of modification at these three different regions is likely important for selective inhibitors[3]. Therefore, discussion as to the selectivity of compounds **1** and **2** for the HDAC6 protein should be more attractive.

In order to explore the vitro HDACs inhibition, all compounds mentioned above (SAHA, MGCD0103, compound **1** and compound **2**) were conducted enzyme inhibitory assays against HDAC1, HDAC2, HDAC3, and HDAC6. Results presented

in Table 2 reveal that two new compounds (compound **1** and compound **2**) exhibited more potent activity against HDAC1, HDAC2, and HDAC3 than the standards (SAHA and MGCD0103). In terms of HDAC6, MGCD0103 with o-aminoanilide moiety has no activity while the other three compounds (SAHA, compound **1**, compound **2**) with hydroxamic acid moiety perform well.

Table 2 In Vitro Inhibition of HDACs Isoforms of SAHA, MGCD0103, Compound **1** and Compound **2** [a]

Compounds	IC_{50} of HDACs（μM）			
	HDAC1	HDAC2	HDAC3	HDAC6
SAHA	0.091	0.193	0.126	0.098
1	0.082	0.187	0.113	0.069
2	0.065	0.134	0.102	0.078
MGCD0103	0.171	0.283	1.165	＞10

[a] Assays were performed in replicate (n≥2); The SD values are < 20% of the mean.

Immunofluorescence microscopy

The HDACs inhibition assay has also been performed using A549 cell line by immunofluorescence microscopy and the result shows consistency with the vitro assay. In accord with SAHA, compound **1** and **2** with hydroxamic acid in the ZBG region markedly increased expression levels of both acetylated tubulin and acetylated histone, implying that the capping and linker group from MGCD0103 cannot contribute to the change of HDAC6 selectivity and o-aminoanilide moiety is a key factor in the selective HDIs.

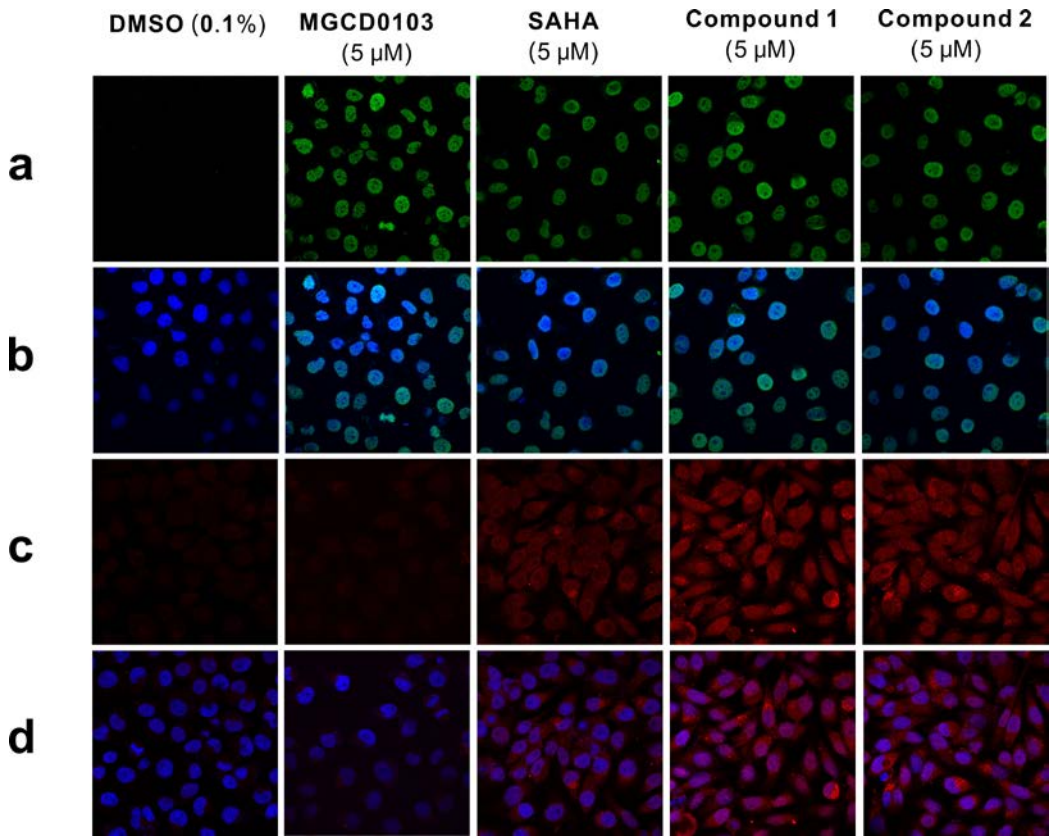

Figure 4

In Vitro Stability Assay

Vitro Stability Assay was also conducted to compare the two compounds and their templates (SAHA and MGCD0103) on stability. P.G Wang had reported that vitro data can provide strong evidence to vivo properties[24]. So based on our vitro data (Table 3), compounds with MGCD0103 Capping Group (compound **1** compound **2** and MGCD0103) were superior to SAHA in half-life potency.

Table 3 In Vitro Stability of SAHA compound **1** compound **2** and MGCD0103

Vitro Conditions	Stability ($t_{1/2}$)			
	SAHA	compound **1**	compound **2**	MGCD0103
Artificial gastric fluid	22h	＞24h	＞24h	＞24h
Artificial intestinal fluid	＞24h	＞24h	＞24h	＞24h
Plasma(mouse)	3h	10h	12h	10h
Micrisome (mouse)	80min	150min	172min	157min

Conclusions

In summary, we focused and investigated on the known clinical HDAC inhibitors, and obtained two potential HDAC inhibitors by fragment-based drug design (FBDD). The two compounds (compound **1** and compound **2**) directly from the optimized scaffolds of known clinical HDAC candidates SAHA and MGCD0103 combined both advantages of them. Based on result of experiments above, they inherited the longer half-life potency derived from MGCD0103 and non-selectivity toward HDAC6 derived from SAHA. To the best of our knowledge, both compounds (compound **1** and compound 2) could be considered as novel histone deacetylase inhibitors in targeted drug development, and possibly anticipated to be more effective under the clinical trials.

Design section

Sixteen known HDAC candidates in the clinical trials, plus compound **24**[25] were selected for the design for novel HDAC inhibitors (Figure 5). Focusing on modifications at the Zn-binding region of these canonical HDAC inhibitors, we step by step replaced this kind of group with three different moieties (hydroxamic acid, o-aminoanilide, and the newly reported 3‑Hydroxypyridin-2-thione2[26]), and finally obtained thirty-four novel HDAC inhibitors.

Molecular docking was widely acceptable for virtual screening in the

fragment-based drug design (FBDD). In this manuscript, we chose three kinds of available HDAC protein crystal complexes (HDAC2, pdb code: 3MAX; HDAC4, pdb code: 2VQW; HDAC8, pdb code: 1W22) as the docking receptors. Subsequently, the thirty-four designed HDAC inhibitors (Figure 5) were docking into the Zn^{2+} ion active pocket of three HDAC proteins, respectively. All the docking studies were performed on the Discovery Studio 3.5 suite. The Consensus Score based on the CDOCKER_INTERACTION_ENERGY of these three HDAC proteins with designed molecules was the final criterion (Table 4). The results showed compounds NH_6, 9, 13 and 16 were ranked in the top of docking energy. Considering the difficulty of the synthesis for these four compounds and reliability of molecule design, we selected NH_16 (compound **1**) as the starting point. Meanwhile, we omitted double bond and shorter the chain length in the structure of compound **1** to obtain compound **2**. As shown in Figure 1, both compounds are fusion of MGCD0103 Capping Group and SAHA Metal-Binding Moiety. MGCD0103 has a longer half-life in plasma ($t_{1/2}$ = 9 h[19]) than SAHA ($t_{1/2}$ = 2 h[18]) while the SAHA Metal-Binding Moiety which is hydroxamic acid has been reported to be interrelated to HDAC6 selectivity[23]. Hopefully, the designed compound **1** and **2** can combine advantages of MGCD0103 and SAHA just like combining their fragments.

To further validate the roles of o-aminoanilide moiety of MGCD0103 and hydroxamic acid moiety of SAHA in the HDAC6 selectivity, we generated the two HDAC6 homology models by comparative protein modeling (modeler) on the ModWeb Server[27], in which Model 1 was built based on the HDAC4 protein crystal complex (PDB code: 4CBT) and the sequence identity was 52% while Model 2 was built based on the a HDAC7 protein crystal complex (PDB code: 3C10) and the sequence identity was 51% (Figure 6a). Docking study of these four compounds on these two protein models were subsequently performed by the CDOCKER algorithm developed on the CHARMM force field[28]. It is noteworthy that the chelating interaction of compounds with the Zn^{2+} ion can play a key role for the binding mode. As observed with the original ligands (9F4 in the 4CBT protein and Trichostatin A in the 3C10 protein), the two oxygen atoms at the hydroxamic acid moiety of the compound **1**, **2**, and SAHA could keep much close to the Zn^{2+} ion, and the distance between O atom and Zn^{2+} ion ranged from 2 to 4 Å (Figure 6b). As to the o-aminoanilide fragment of MGCD0103, although some model[12] showed that the carbonyl-oxygen and the ortho-NH2 groups could directly interact with the Zn^{2+} ion

and the distance between the carbonyl-oxygen and Zn^{2+} ion on the Model 1 protein was much closer, just 2.2 Å, this kind of moiety actually could not be accommodated well in the HDAC6 deep pocket. For example, the binding mode on the Model 2 protein seemed very impractical, in which the distance between the carbonyl-oxygen and Zn^{2+} ion was 6.1 Å (Figure 6b). Moreover, the docking energy of these four compounds were ranked, and indicated that SAHA, compound **1** and **2** can prefer HDAC6 protein.

In summary, we cut clinical drugs into fragments and generate new compounds by structural manipulations, including linking, merging and growth. With the process of molecular docking, two compounds (compound **1** and compound **2**) stood out. And then HDAC6 homology models are generated to validate their HDAC6 selectivity. While SAR of clinical drugs as well as its fragments has been discussed before, our design leads to further optimization of selectivity and half-life potency. These two compounds designed are expected to have longer half-life potency like MGCD0103 and extensive inhibition against HDACs like SAHA.

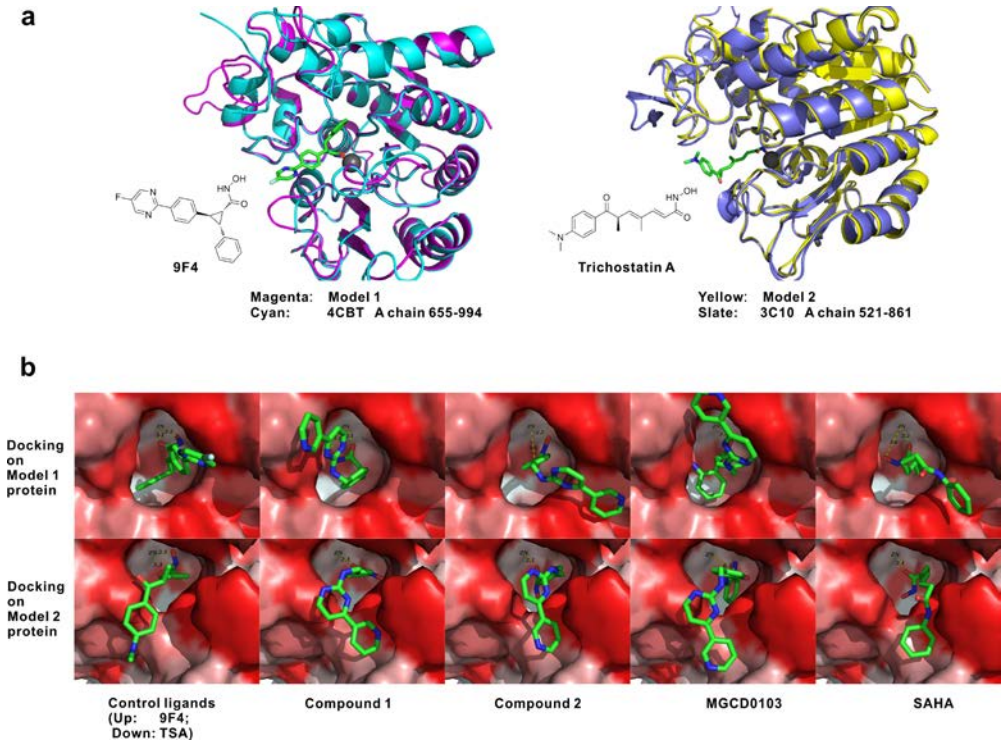

Figure 6

Chemistry section

The synthesis of compound **1** and compound **2** is described in scheme 1. Synthesis of compound **B** was started with 3-(dimethylamino)-1-(pyridin-3-yl) prop-2-en-1-one (compound **A**) and guanidine hydrochloride being mixed in Bu-OH, then being heated to reflux for overnight. With the reaction of nucleophilic replacing, compound **C** and compound **D** were given respectively from compound **B**. Compound **C** was further subjected to Heck reaction and gave compound **E**. Compound **F** was simply got by hydrolysis reaction from compound **D**. At the same condition, Compound **E** and Compound **F** were converted to the target hydroxamic acid Compound **1** and Compound **2** respectively.

Scheme1. The synthesis routes of compound **1** and **2**

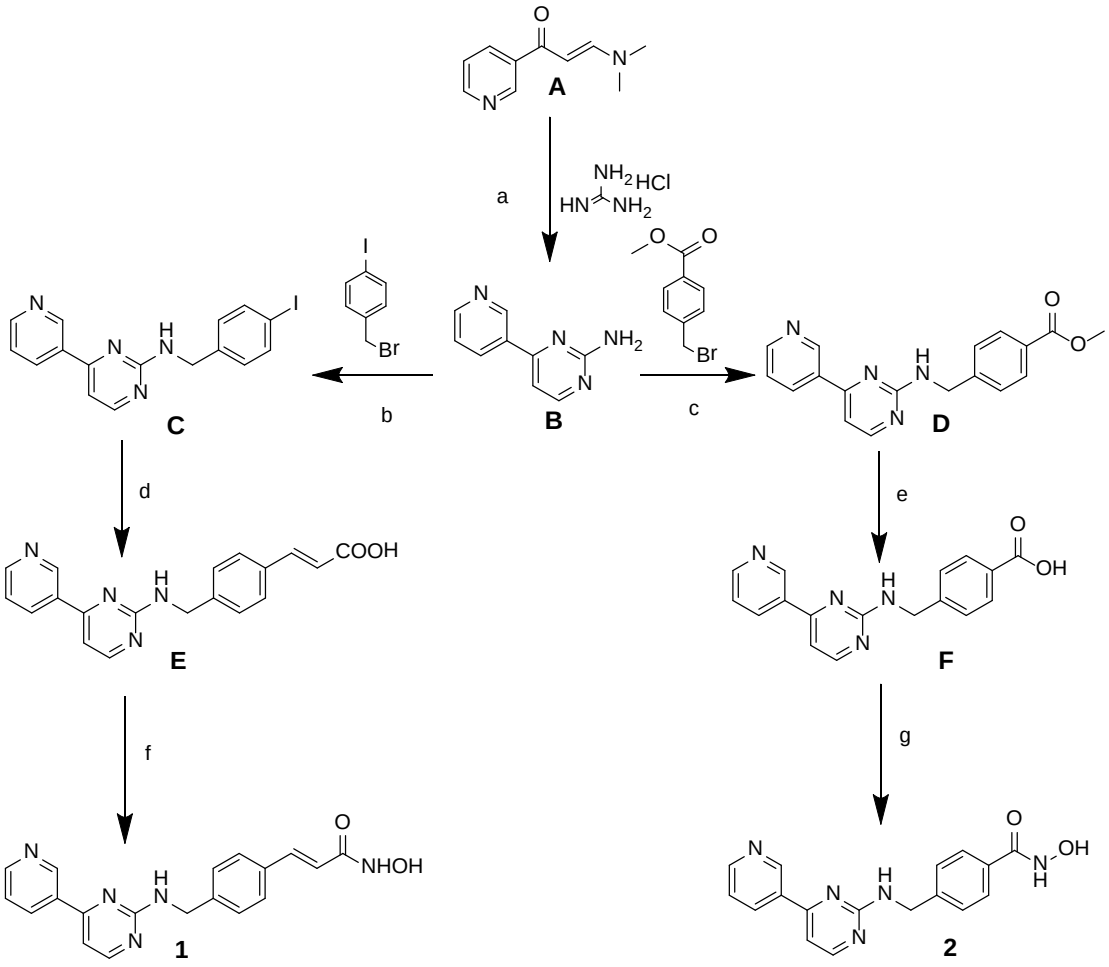

Conditions: a) NaOH, n-BuOH, reflux, overnight; b/c) NaH, THF, rt, 8h; d) CH_2=CHCOOH, $Pd_2(bda)_3$, POT, Et_3N, DMF, 100 ℃, overnight; e) MeOH, H_2O,

NaOH, HCl, rt, 2h; f/g) NH_2OTHP, EDC, HOBt, DMF, 50 ℃, 6h.

Biological section

Antiproliferative Assay by the MTT method

All cells lines (A549, Hela, HepG2, HCT116, and MCF-7) were maintained in DMEM or RPMI-1640 medium containing 10% fetal bovine serum at 37 ℃, in a 5% CO_2 humidified incubator. Cell proliferation assay was determined by the MTT method. Briefly, cell lines were passaged the day before seeding into 96-well plates, allowed to grow for 12h, and then treated with different concentrations of compounds for 24h, 48h, 72h respectively. A 5 mg/ml MTT solution was added to each well. After incubation for another 4h, media inside was carefully removed and 100μL DMSO was added. Rocking for 15min later, absorbance was determined using an ELISA reader at 570nm. Each well should be kept at least three parallel experiments, and Dose-dependent curves were calculated by Origin 8.6. The detailed results were displayed in Supplementary Information Figure s5.

Induced apoptosis by Flow Cytometry

To detect apoptosis induced by compound **1** and **2**, Hela cells were seeded per well in 24-well plates and were incubated overnight. Then cells were treated with compound **1** and **2** at the three different concentrations (1.25 μM, 2.5 μM and 5 μM, separately). MGCD0103 and SAHA were chosen as positive controls and DMSO was chosen as the negative control. After 48 h, cells were harvested for the apoptosis detection. In brief, collected cells were washed once with PBS and subsequently washed once with binding buffer, and then stained with FITC conjugated Annexin V and propidium iodide (PI) in the binding buffer for 20 min at room temperature in the dark. Apoptotic cells were quantified using a FAC Scan cytofluorometer (PT. Madagasi Brosa Inc. JI. Batang Hari NO.73, Propinsi Sumatera Utara, Indonesia) plotting at least 10,000 events per sample. To quantify the data, the frequencies in all quadrants were analyzed using flowjo software. We regarded cells in the lower right quadrant (Annexin V positive / PI negative) as early apoptotic cells, and cells in upper right quadrant (Annexin V positive / PI positive) as late apoptotic cells and necrotic cells.

Cell cycle assay by Flow Cytometry

To detect the effect of the compound **1** and **2** on cell cycle, Hela cells were treated with compound **1** and **2** at the gradient concentrations (0.5 μM, 1 μM and 2 μM), and DMSO was used as the negative control. After 24 h, cells were harvested, washed with PBS once, and fixed in PBS containing 75% ethanol at -20℃ overnight. Then cells were collected by centrifugation, and subsequently resuspended in PBS containing 0.1 mg/mL RNase A and 5 μg/mL propidium iodide (PI) and kept in the dark for 30 min before the cell cycle detection. Cellular DNA content, for cell cycle distribution analysis, was measured by flow cytometry using FAC Scan cytofluorometer plotting at least 10,000 events per sample. The percentage of cells in the G0/G1, S and G2/M phases of the cell cycle were determined using modfit software.

Vitro HDACs Inhibition Fluorescence Assay

Firstly, 10 μL of enzyme solution (Hela nuclear extract, HDAC1, HDAC2, HDAC3 or HDAC6) and various concentrations of four compounds (SAHA, MGCD0103, compound **1** and compound **2**) were mixed. The mixture was incubated at 37℃ for 5 min, and then luorogenic substrate Boc-Lys(acetyl)-AMC (40μL) was added. After being incubated at 37℃ for 30 min, the mixture was stopped by adding 100μL of developer containing trypsin and TSA. 20 min later, fluorescence intensity was measured using a micro plate reader at excitation and emission wavelengths of 390 and 460 nm, respectively. The inhibition ratios were calculated from the fluorescence intensity readings of tested wells relative to those of control wells, and the IC_{50} values were calculated using a regression analysis of the concentration /inhibition data.

Immunofluorescence microscopy procedures

A549 cells were seeded on cover slips and incubated at 37 ℃. After 24 h , the media was replaced with media containing 0.1% DMSO, or the dilution with test compounds (5 μM SAHA, 5 μM MGCD0103, 5 μM compound **1**, 5 μM compound **2**) containing 0.1% DMSO, and incubated at 37 ℃. After 24 h, the cells were fixed (see below for fixation protocols) and incubated with antibodies and stains (see below for antibody detection and staining protocols). All the images were captured on a Nikon confocal microscope (C2+, Nikon, Tokyo, Japan) and analyzed using Nis-element advanced research software (Nikon).

Fixation Protocols

Tubulin

The media was aspirated and the cover slips incubated 400 μL fixation solutions (4% glutaraldehyde solution of PBS) for 20 min. The fixation solution was then aspirated and the cover slip rinsed with PBS/0.1% Triton-X-100 for 3×5 min. The cover slip was then incubated with 300 μL of a 10 mg/mL sodium borohydride solution in PBS for 10 min. This solution was aspirated, and the cover slip rinsed with 400 μL PBS for 3×5 min. The cover slip was then blocked with 2% bovine serum albumin for 10 min.

Histone

Media was aspirated and replaced with 300 μL 5% acetic acid/ethanol (-20 °C) and this incubated 3 min. The acetic acid/ethanol solution was then aspirated and the cover slip rinsed with PBS. The cover slip was then incubated with 300 μL PBS/0.5% Triton-X-100 for 10 min. This solution was then aspirated and the cover slip blocked with 2% bovine serum albumin for 10 min.

Antibody Detection/Staining Protocol

Cover slips fixed for optimal tubulin visualization were incubated with anti-acetylated tubulin antibody (Sigma monoclonal clone 6-11B-1) in BSA (1:300 dilution) for 1 h at 37 ℃. Cover slips fixed for optimal histone visualization were incubated with anti-acetylated lysine antibody (Cell Signaling monoclonal Ac-K-103) in BSA (1:200 dilution) for 1 h at 37 ℃. Cover slips were then washed 3×5 min with 300 μL PBS/ 0.1% Triton-X-100. Cover slips were then incubated with secondary antibody (1:400 Molecular Probes Alexa Fluor® 594 goat anti-mouse IgG in BSA for tubulin and 1:200 Molecular Probes Alexa Fluor® 488 goat anti-mouse IgG in BSA for histone) for 1 h at 37 ℃ in the dark. After subsequent washing (3×5 with 400 μL PBS/ 0.1% Triton-X-100), all cover slips were stained with DAPI staining solution (Beyotime 10 mg/mL stocked diluted 1:1000 in BSA) for 20 min in dark. All cover slips were then washed extensively in the dark (3×5 min with 300 µL PBS, 1×5 min with 300 μL ddH_2O) prior to mounting.

Homology and Molecular Modeling

Homology Modeling

Human HDAC6 sequences were obtained from the NCBI database (http://www.ncbi.nlm.nih.gov/protein/AAH69243.1). Due to the HDAC6 has two catalytic subunits, we chose the second one (CDII, Gly482-Gly800) as the major functional domain in the HDAC6 protein. In the next step, we submitted this sequence into the ModWeb server maintained by Sali group (https://modbase.compbio.ucsf.edu/modweb/). It was noted that we chose the "Slow (Seq-Prf, PSI-Blast) as Fold assignment methods that make our model more accurate. Two models (Model 1 and 2) have been obtained, in which Model 1 was built on the HDAC4 protein crystal complex (PDB code: 4CBT) as the template, and the sequence identity was 52% while Model 2 was built on the HDAC7 protein crystal complex (PDB code: 3C10) as the template, and the sequence identity was 51%.

To adjust the position of zinc at the catalytic site, Model 1 was superimposed over the crystal structure of 4CBT by protein structure similarity method of the Discovery Studio 3.5 suite while Model 2 was superimposed over the crystal structure of 3C10 in the same way. Finally, an energy minimization was performed and the homology modeling procedure was completed.

Molecular Docking

Molecular docking of compounds into the three dimensional protein structure of human HDAC6 (Model 1 and 2) was carried out using the Discovery Studio (version 3.5) as implemented through the graphical user interface DS-CDOCKER protocol. The three-dimensional structures of the aforementioned compounds were constructed using Chem. 3D ultra 12.0 software [Chemical Structure Drawing Standard; Cambridge Soft corporation, USA (2010)], then they were energetically minimized by using MMFF94 with 5000 iterations and minimum RMS gradient of 0.10. All bound waters and ligand were eliminated from the protein and the polar hydrogen was added to the proteins. Each compound would retain 20 poses, and was ranked by CDOCKER ENERGY. The selection of the conformation of each compound would partly depend on the binding mode in the active pocket, when compared to those known control such as 9F4 and TSA.

Reference

1. Khan, O. & La Thangue, N. B. HDAC inhibitors in cancer biology: emerging mechanisms and clinical applications. *Immunol. Cell. Biol*. **2012**, 90, 85-94.
2. Clayton, A. L. *et al.* Enhanced histone acetylation and transcription: a dynamic perspective. *Mol. Cell*. **2006**, 23, 289-296.

3. Bieliauskas, A. V. & Pflum, M. K. Isoform-selective histone deacetylase inhibitors. *Chem. Soc. Rev*. **2008**, 37, 1402-1413.
4. Benedetti, R. *et al.* Targeting Histone Deacetylases in Diseases: Where Are We? *Antioxid. Redox. Signal*. **2014**.
5. Marks, P. A. & Breslow, R. Dimethyl sulfoxide to vorinostat: development of this histone deacetylase inhibitor as an anticancer drug. *Nat. Biotechnol*. **2007**, 25, 84-90.
6. Campas-Moya, C. Romidepsin for the treatment of cutaneous T-cell lymphoma. *Drugs of today (Barc)*. **2009**, 45, 787-795.
7. David C. Rees, Miles Congreve, Christopher W. Murray, Robin Carr. Fragment-based lead discovery. *Nat. Rev. Drug Discovery.* **2004**, 3, 600-672.
8. Philip J. Hajduk, Jonathan Greer. A decade of fragment-based drug design: strategic advances and lessons learned. *Nat. Rev. Drug Discovery.* **2007**, 6, 211-219.
9. Hou J., *et al,* Discovery and extensive in vitro evaluations of NK-HDAC-1: a chiral histone deacetylase inhibitor as a promising lead. *J Med Chem*. **2012**, *55*, 3066-3075.
10. Tung TT., *et al,* New benzothiazole/thiazole-containing hydroxamic acids as potent histone deacetylase inhibitors and antitumor agents. *Med Chem*. **2013**, *9*, 1051-1057.
11. Witter DJ., *et al,* Benzo[b]thiophene-based histone deacetylase inhibitors. *Bioorg Med Chem Lett*. **2007**, *17*, 4562-4567.
12. Hooven LA., *et al,* Effects of suberoylanilide hydroxamic acid and trichostatin A on induction of cytochrome P450 enzymes and benzo[a]pyrene DNA adduct formation in human cells. *Bioorg Med Chem Lett*. **2005**, *15*, 1283-1287.
13. Chan CT. *et al,* Syntheses and discovery of a novel class of cinnamic hydroxamates as histone deacetylase inhibitors by multimodality molecular imaging in living subjects. *Cancer Res*. **2014**, *74*, 7475-7486.
14. Ning C., *et al,* Design, synthesis and biological evaluation of di-substituted cinnamic hydroxamic acids bearing urea/thiourea unit as potent histone deacetylase inhibitors. *Bioorg Med Chem Lett*. **2013**, *23*, 6432-6435.
15. Hou J., *et al,* Structure-based optimization of click-based histone deacetylase inhibitors. *Eur J Med Chem*. **2011**, *46*, 3190-3200.
16. Chen L., *et al,* Dual inhibitors of inosine monophosphate dehydrogenase and histone deacetylase based on a cinnamic hydroxamic acid core structure. *Bioorg Med Chem*. **2010**, *18*, 5950-5964.
17.Dallavalle S., *et al,* Design, synthesis, and evaluation of biphenyl-4-yl-acrylohydroxamic acid derivatives as histone deacetylase (HDAC) inhibitors. *Eur J Med Chem*. **2009**, *44*, 1900-1912.
18. Rubin, E. H. *et al.* A study to determine the effects of food and multiple dosing on the pharmacokinetics of vorinostat given orally to patients with advanced cancer. *Clin. Cancer. Res*. **2006**, 12, 7039-7045.
19. Garcia-Manero, G. *et al.* Phase 1 study of the oral isotype specific histone deacetylase inhibitor MGCD0103 in leukemia. *Blood*. **2008**, 112, 981-989.
20. Marks, P. A. Discovery and development of SAHA as an anticancer agent.

Oncogene. **2007**, 26, 1351-1356.
21. Ververis, K. *et al.* Histone deacetylase inhibitors (HDACIs): multitargeted anticancer agents. *Biol. Tar. Ther.* **2007**, **7**, 47-60.
22. Lane, A. A. & Chabner, B. A. Histone deacetylase inhibitors in cancer therapy. *J. Clin. Oncol*. **2009**, 27, 5459-5468.
23. Wong, J. C. *et al.* Structural biasing elements for in-cell histone deacetylase paralog selectivity. *J. Am. Chem. Soc*. **2003**, 125, 5586-5587.
24. Wang, P. G. *et al.* Discovery and extensive in vitro evaluations of NK-HDAC-1: a chiral histone deacetylase inhibitor as a promising lead. *J. Med. Chem*. **2012**, 55, 3066-3075.
25. Marson, C. M. *et al.* Discovery of potent, isoform-selective inhibitors of histone deacetylase containing chiral heterocyclic capping groups and a N-(2-aminophenyl)benzamide binding unit. *J. Med. Chem*. **2013**, 56, 6156-6174.
26. Patil, V. *et al.* 3-Hydroxypyridin-2-thione as novel zinc binding group for selective histone deacetylase inhibition. *J. Med. Chem*. **2013**, 56, 3492-3506.
27. Wu, G. *et al.* Detailed analysis of grid-based molecular docking: A case study of CDOCKER-A CHARMm-based MD docking algorithm. *J. Comput. Chem*. **2003**, 24, 1549-1562.
28. Pieper, U. *et al.* ModBase, a database of annotated comparative protein structure models, and associated resources. *Nucleic. Acids. Res*. **2011**, 39, D465-474.

Acknowledgements

This work was supported by Natural Science Foundation of Jiangsu Province (No. BK20130554) and by Major Projects on Control and Rectification of Water Body Pollution (2011ZX07204-001-004).

Supplementary Information Chemistry details for the synthesis two target compounds and Figures for ^{1}H NMR, ESI and antiproliferative assay.

Abbreviations

FBDD, fragment-based drug design;

HDIs, Histone deacetylase inhibitors;

HDAC, Histone deacetylase;

HAT, Histone acetyltransferase;

ZBG, Zn-binding group;

TSA, Trichostatin A.

Corresponding Author

*Tel.: +86-25-83592572; Fax: +86-25-83592672; E-mail address: zhuhl@nju.edu.cn.

Competing financial interests

The authors declare no competing financial interest.

Figures, Tables and Scheme (**caption**s)

Figure1. Targeted compounds **1** and **2** obtained by visual screening. These two compounds were assembled by employing the ZBG moiety of SAHA, and the Cap and linker fragment of MGCD0103. Classification of HDAC chemical space from SAHA to MGCD0103 was subjectively based on the analysis of recently published HDAC inhibitors paper.

Figure2. Apoptosis assay on human caner Hela cells by flow cytometry. Four compounds (MGCD01013, SAHA, compound **1** and **2**) were used at three different doses (A: 1.25μM, B: 2.5μM, C: 5μM).

Figure3. Cell cycle profiles of compound **1** and **2** on Hela cells at three different doses (0.5, 1, and 2μM, respectively).

Figure4. Immunofluorescence microscopy detection in A549 cells of acetylated histones (row a); acetylated histones and DAPI nuclear staining (row b); acetylated tubulin (row c); acetylated tubulin and DAPI nuclear staining (row d). Cells were treated for 12 h with the indicated compound (columns).

Figure5. Designed small molecule HDAC inhibitors based on Clinical candidates except compound **24a**.

Figure6. The results of homology modeling and molecular docking on HDAC6 protein (a)Two homology models of HDAC6 by the ModWeb Server in SALI lab (Modeller): one template is the continuous segment of residues between 655 and 994 of the A chain of 4CBT, a HDAC4 protein crystal complex with a small molecule 9F4 in the protein data bank (PDB); the other one is the continuous segment of residues between 521 and 861 of the A chain of 3C10, a HDAC7 protein crystal complex with a small molecule Trichostatin A (TSA) in the protein data bank (PDB); (b) Docking

modes of compound **1**, **2**, MGCD0103, and SAHA based on Model 1 and Model 2; All the figures were drawn by Pymol 1.6, and red regions represented hydrophobic surface.

Table1. Antiproliferative activities of the designed compounds against five common cancer cells

Table2. In Vitro Inhibition of HDACs Isoforms of SAHA, MGCG0103, Compound **1** and Compound **2**

Table 3 In Vitro Stability of SAHA compound **1** compound **2** and MGCD0103

Table 4. Results of virtual screening by molecular docking based on three human HDAC protein crystal structures (HDAC2, pdb code: 3MAX; HDAC4, pdb code: 2VQW; HDAC8, pdb code: 1W22)

Table 5. The docking energy of MGCD0103, SAHA, compound **1** and **2** on the homology modeling of HDAC6

Scheme1. The synthesis routes of compound **1** and **2**

Figure5. Designed small molecule HDAC inhibitors based on Clinical candidates except compound **24a**.

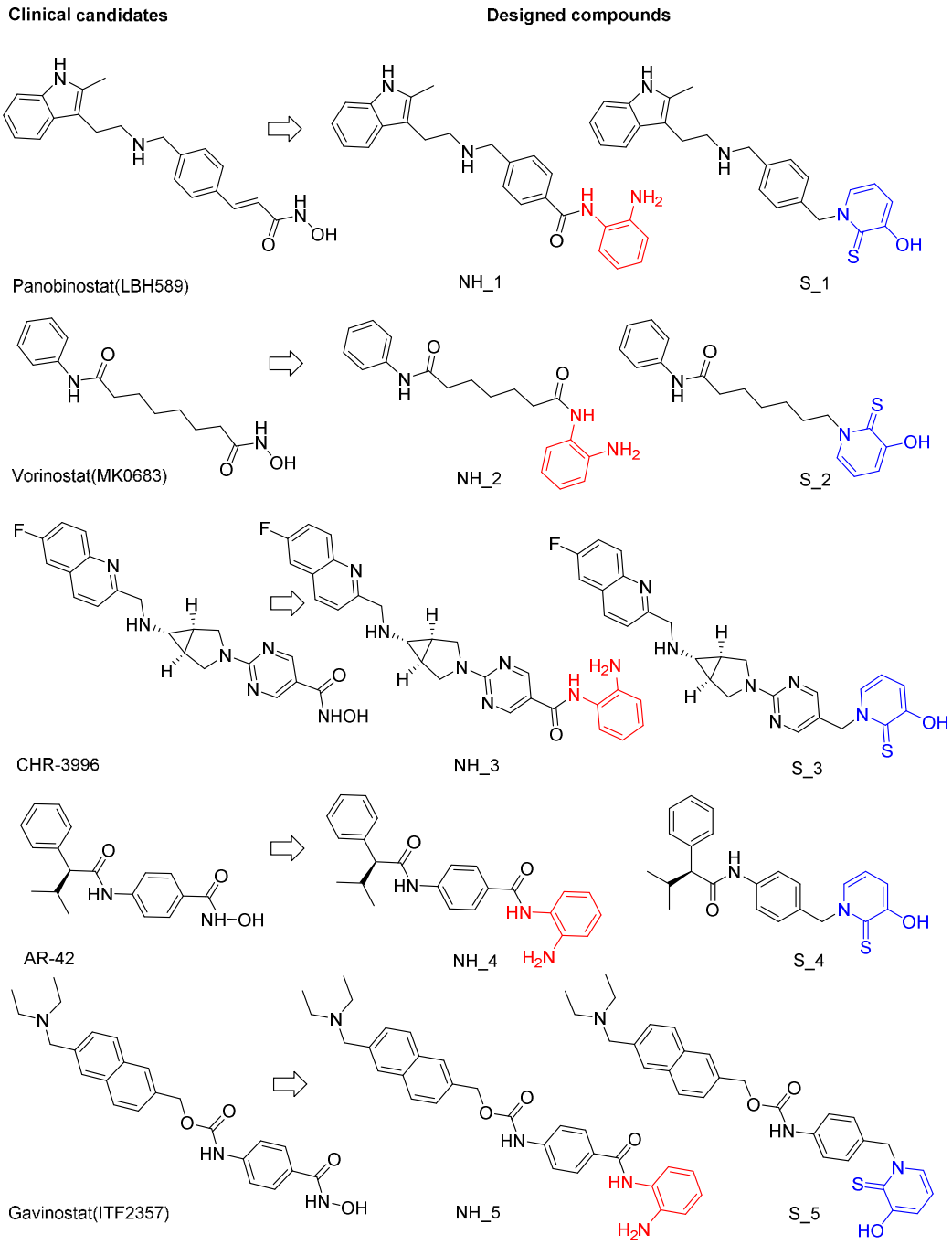

Figure 5 Continue;

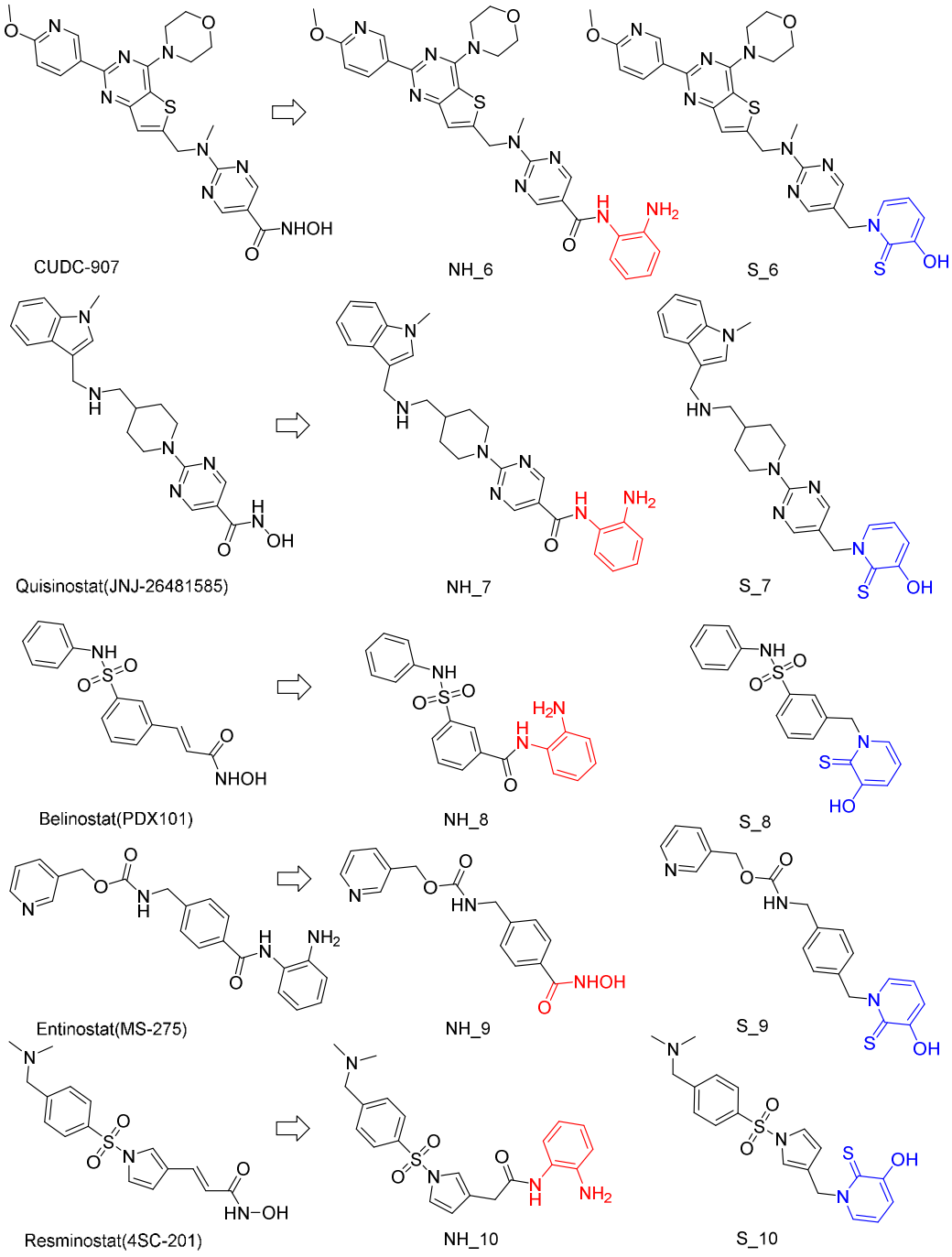

Figure 5 Continue;

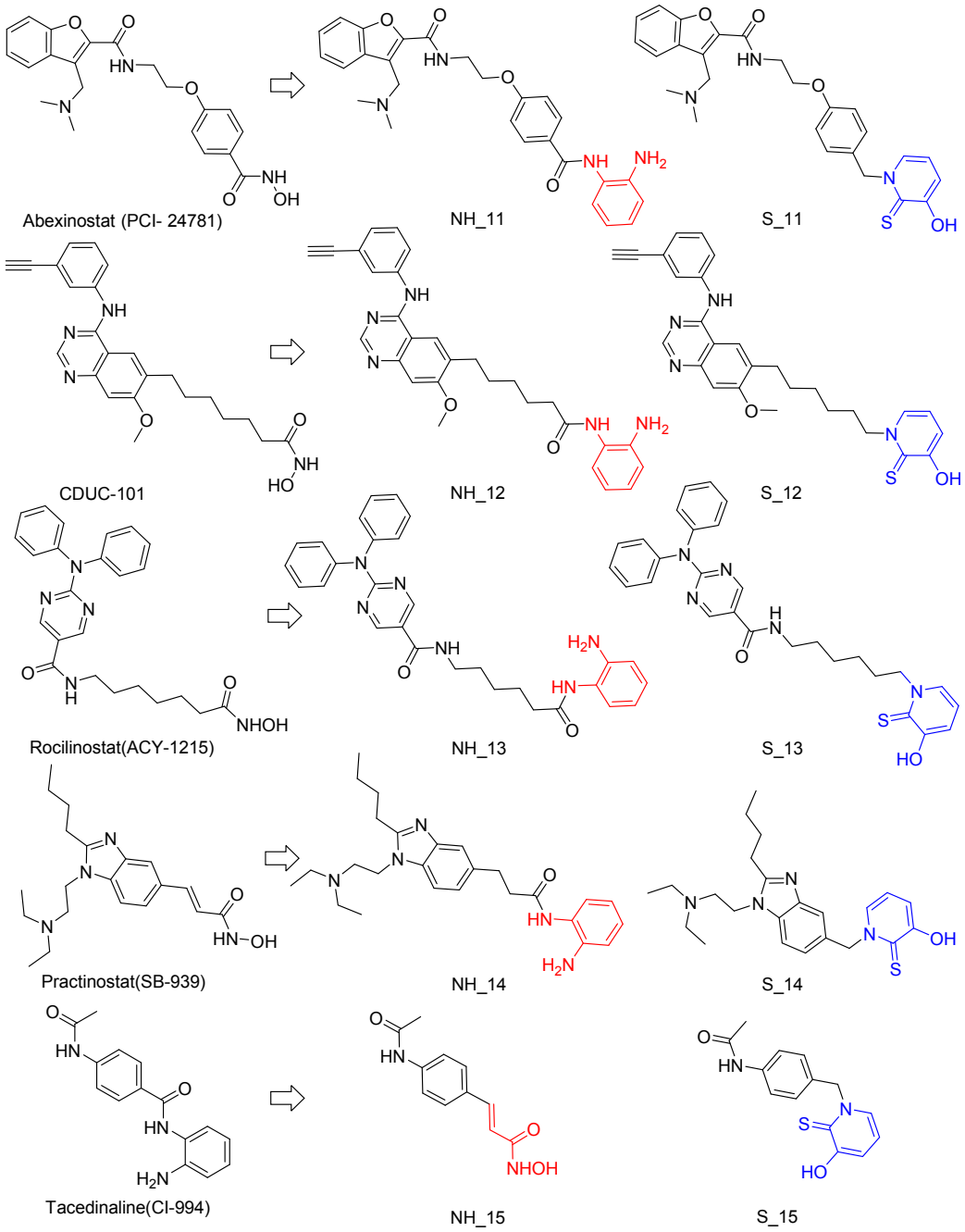

Figure 5 Continue;

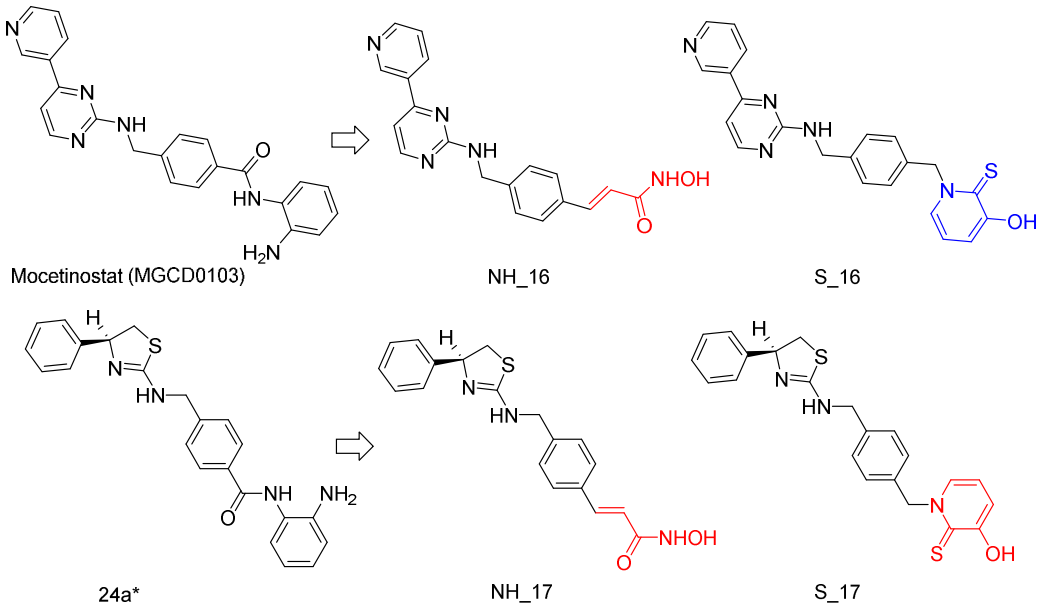

* referred to that this compound was abstracted from ref 1.

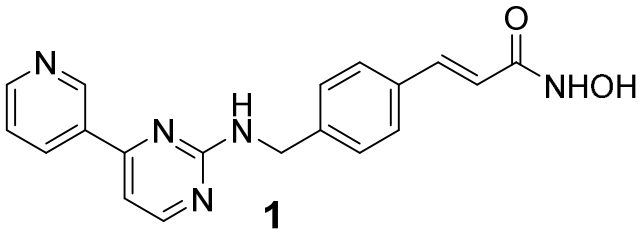

1

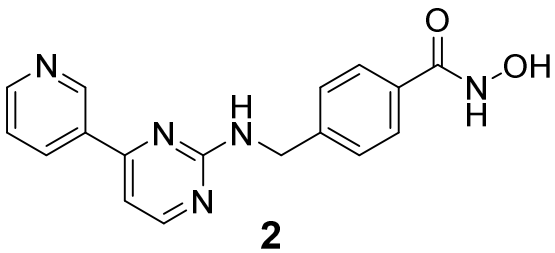

2

Navigating into chemical space between MGCD0103 and SAHA using two novel histone deacetylase inhibitors